Journal of Civil Engineering and Construction 2024;13(3):134-145
https://doi.org/10.32732/jcec.2024.13.3.134

Variation of Shear Strength of Cohesive Soils Subjected to Cyclic Loading at Different Rates of Loading

Aseel N. Najim, Mohammed Y. Fattah*, Makki K. M. Al-Recaby

Civil Engineering Department, University of Technology, Baghdad, Iraq
E-mail: aseelnabeel92@yahoo.com; 40011@uotechnology.edu.iq (Corresponding author); 40139@uotechnology.edu.iq.

Received: 2 February 2024; Accepted: 22 May 2024; Available online: 15 July 2024

Abstract: There is a dearth of research on the cyclic vertical loading problem for cohesive soil, with the majority of studies conducted in commercial settings. The purpose of this work is to investigate the experimental effects of vertical cyclic compression stress on the undrained shear strength of clayey soil. To investigate the undrained shear strength of clays beneath shallow footings under cyclic loads at various rates, thirty-nine models have been put to the test. A brand-new compression device was produced with the ability to apply both cyclic and monotonic loading. Two footing shapes, three depths of foundation embedment, three undrained shear strengths, and three loading rates were tested. It was determined that following the cyclic load test, the soil's undrained shear strength increased in value. At the start of the test, there was a sharp rise in settlement. This indicates that in all models, the threshold stain is extremely tiny in the zones of cyclic amplitudes.
Keywords: Cohesive soil; Cyclic load; Rate of loading; Undrained shear strength**.**

1. Introduction

In geotechnical engineering, determining the reduction of static undrained shear strength is crucial. It is also vital to determine the post-cyclic undrained shear strengths of low plastic silty clays and clayey silts and compare the outcomes with the pre-cyclic condition. Additionally, the impact of specimen type and soil plasticity on the post-cyclic shear strength behavior and dynamic shear strength of fine-grained soils were investigated. Following the earthquakes, field conditions and damaged areas were observed. These observations revealed that, under cyclic loadings, bearing failure occurs in low plastic silty and clayey soils due to the limited amount of pore water pressure caused by ground softening and the rapid increase in shear strains [1, 2].

Despite being categorized as fine-grained soils, silts can behave differently cyclically than clays. The flexibility of the fines content determines the differences in the cyclic shear strength properties and the pore water pressure response during cyclic loading. In plastic silty clays, pore pressure can rise to a certain point, but in saturated sandy silts and silty sands, it can achieve the effective confining pressure in a single loading cycle. As a result, the soils undergo significant deformation as a result of the quick rise in pore water pressure, which lowers the effective stresses that lead to soil liquefaction [3 - 5].

One of the key factors influencing the cyclic behavior of undisturbed silty soils is the flexibility of the fines content [6 - 8]. Compared to plastic silts, undisturbed non-plastic silts have a lower cyclic strength. Puri [9] used cycle triaxial testing on reconstituted soil specimens to examine the impact of the plasticity index on the cyclic undrained shear strength of typically consolidated silty soils. Based on the findings, it was concluded that for a given number of cycles, an increase in the plasticity index causes a considerable increase in the shear stress ratio that results in 5% twofold amplitude shear strain.

According to Ansal and Erken [10], there is a crucial cyclic shear strain level at which soils experience significant deformations every cycle. This level is known as the cyclic yield strength level.

Boulanger and Idriss [11] defined the terms "sand-like" for liquefaction and "claylike" for cyclic failure to characterize the cyclic behavior of fine-grained soils. There appears to be a threshold value for the plasticity index of clay fractions, below which the liquefaction resistance drops and beyond which the liquefaction resistance begins to increase, based on the majority of prior research and a careful analysis of pertinent data from the literature. Furthermore, the study has examined the cyclic strength (τ_{cyc}) of clay-like fine-grained soils, standardized by monotonic undrained shear strength (s_u), taking into account many aspects including test type, over consolidation ratio, and plasticity index. It was indicated that for naturally clay-like soils subjected to simple shear loading, the τ_{cyc}/s_u ratio for number of cycles N = 30 is taken as 0.83.

Since the early 1980s, a number of researchers have examined the post-cyclic behavior of fine-grained soils. The loss of static undrained shear strengths of softening soils beneath building foundations is included in these investigations. Indeed, it would be a reasonable assumption to state that the soils with no post-cycle strength are those subjected to residual strains from cyclic loadings [12].

Finn [13] assessed how earthquake pressures affected the soil's remaining undrained shear strength through the shear surface. It was concluded that a confining pressure correction should be applied while performing a soil stability study at the limit state condition. Vasquez-Herrera and Dobry [14] as well as Marcuson et al. [15] investigated the post-cyclic strength of soils. Several laboratory experiments were conducted to ascertain the residual strengths of the soil specimens removed from the San Fernando Dam's hydraulic fill. Following that, a comparison was made between the test findings and the field strategy derived from the standard penetration levels.

Undrained cyclic triaxial tests were conducted by Li et al. [16] on soft clays originating from the maritime environment in Wenzhou, China. It was determined that at lower frequencies, greater pore pressures and shear strains were produced. There is a significant reduction in the number of cycles needed to attain failure when the frequency drops from 1 Hz to 0.01 Hz.

The experimental behavior of dry sandy soil under foundations subjected to vertical cyclic compression load was investigated by Fattah et al. [17]. In order to investigate the behavior of shallow footings under cyclic loads at various rates, sixty-three models have been evaluated. A brand-new compression device was produced with the ability to apply both cyclic and monotonic loading. We experimented with two footing shapes, three relative densities of sand, three depths of foundation embedment, and three loading rates. It was determined that soil settlement decreases with increasing footing depth (D_f). Generally speaking, the soil's bearing capacity improves as the depth or width of the foundation grows, provided that all other variables stay the same. Over the course of the load, a footing's total settlement increases and reaches its maximum value at the conclusion of the dwell time. To some extent, the footing rebounds during the load's decay period. The density of the sand substrate determines how the loading rate acts. The cyclic load settling in dense sand reduces with the rate of loading, whereas in loose sand, it increases with the rate of loading.

Nine models representing layers beneath flexible pavement layers of subgrade and subbase layers were prepared for a testing program by Fattah et al. [18]. The models had dimensions of 800 x 800 x 800 mm, with a 400 mm thick subgrade layer and a 300 mm thick subbase layer. Geogrid reinforcement is used in the center of the subbase layer and at the interface between the subgrade and subbase layer as part of the model tests. The tests were performed in three different configurations: under cyclic load, in saturation testing, and after a 24-hour saturation interval. It was determined that, when compared to an unreinforced subbase layer on expansive subgrade soil, the load carrying capability of the pavement system increases significantly for geogrid reinforced subbase stretch. The model subjected to cyclic load at the interface between the saturated subbase and the subgrade layer, reinforced with geogrid, exhibits the least displacement and transfers the most load. This model's displacement is reduced by roughly 4.5–5.0% when compared to the unreinforced model, but the third model only demonstrated a displacement reduction of roughly 3-3.5%.

In soft soil, long-term cyclic loads applied at a stress level below the critical cyclic stress can cause soil deformation but not failure. Ren et al. [19] presented a unique empirical model with three parameters based on an analogous study of the Monismith and Hardin Drnevich models. The experimental data from the literature was used to validate the suggested model, which was found to perform better than the Monismith model in forecasting the cumulative plastic strain of soft soil under low cyclic loads over an extended period of time. It was suggested that parameter b should have a value of 0.5. Additionally, correlations between parameters a and c and the cyclic stress ratio are suggested for soft clay. The suggested model's applications are explained in detail, and its effectiveness is assessed using the findings of in situ tests conducted on soft subgrade settling. The test findings and the predicted results agreed. The findings of the study offer a viable approach for examining how wave and/or traffic stresses induce soft foundation to settle and develop deformation in near-shore and offshore regions.

When both monotonic shear stresses (τ_o) and cyclic shear stresses (τ_c) are applied to a soft cohesive soil, Patiño et al. [20] referred to the cyclic shear strains (γ_c) and permanent shear strains (γ_p). Tests in the lab were conducted on undisturbed materials, and the results showed that the monotonic strength (τ_{max}) was roughly 30% of the initial effective vertical stress (σ'_{vo}). The findings showed that: (a) the generation of γ_c and γ_p is controlled by the combination of τ_o and τ_c; (b) the cyclical failure of the soil occurs when $\tau_o/\sigma'_{vo} + \tau_c/\sigma'_{vo} \approx \tau_{max}/\sigma'_{vo}$; and (c) the number of cycles (N), for various relationships varying (τ_o/σ'_{vo}) between 0% and 25%.

The impact of loading circumstances and stress history on the failure characteristics and dynamic behavior of cohesive soil with minimal plasticity was assessed by Thakur et al. [21]. Triaxial controlled cyclic testing with two-way strain were conducted. For cyclic axial strain amplitude (ε_a) fluctuation of 0.5%, 1%, 1.5%, and 2%, and OCR values of 1-4, the impact of stress history and loading circumstances was assessed on low plasticity soil. Even at lower amplitude and higher OCR, liquefaction of the low plasticity soil was seen. It was found that soil's liquefaction resistance increased with OCR (1–4) increased and decreased as cyclic strain amplitude (0.5%–2.0%) increased. At pore pressure ratio (r_u) of 0.85, the rate of stiffness degradation showed a bilinear response.

The objective of the present study is to investigate the effect of cyclic loading on the shear strength of cohesive soils. The shear strength shall be measured before loading and after a number of load cycles.

2. Experimental work

2.1 Index properties of soil

A brown clayey soil was brought from a site south of Baghdad city in Iraq. Standard tests were run to ascertain the soil's physical characteristics. Table 1 provides details. The soil is categorized as (CL) by the Unified Soil Classification System (USSCS).

Table 1. Physical properties of the clayey-soil.

Test	Value	Specification
Liquid limit (LL), %	43	ASTM D 4318-(2010) [22]
Plastic limit (PL), %	19	ASTM D 4318-(2010) [22]
Plasticity index, %	24	ASTM D 4318-(2010) [22]
Specific gravity (Gs)	2.67	ASTM D 854-(2010) [23]
Gravel %, > 4.75 mm	0	ASTM D 422-(2010) [24]
Sand %, 0.075-4.75 mm	3	ASTM D 422-(2010) [24]
Silt %, 0.005-0.075 mm	35	ASTM D 422-(2010) [24]
Clay %, < 0.005 mm	62	ASTM D 422-(2010) [24]
Activity	0.39	-

2.2 Design and fabrication of load setups

Two pneumatic cylinders comprise the loading system: Cylinder 1 can apply loads ranging from 153.72 N to 442.00 N, while Cylinder 2 can handle medium and high range loads up to 1170 N. The compressor is composed of aluminum, and the washer-packing (content pressure) is composed of Viton. Two cylinders with pneumatic valves are connected by a flexible hose. With the two cylinders mounted on top of the device's upper-pressure plate with d=14 mm, a different shaft is utilized. It moves up and down with (cylinder piston movement) and is used to stop the footing from rotating.

One of the following options may be selected based on the force imparted to the footing when a cyclic or static load is applied: one of the cylinders.

2.2.1. Control System

As seen in Figure 1, this system is utilized to regulate the device's movement when loads—cyclic or monotonic—are applied. These valves are operated by an electric panel. This panel can be operated manually with two buttons—one to move upward and the other to move downward—or automatically with the help of relays and a timer. To use the gadget in monotonic or cyclic mode:

1) First, the electric switch is swapped out with a manual switch, and the necessary movement is measured up or down. Next, the external timer on the panel interface is used to establish the time. There is a maximum time limit of 996 seconds, or sixteen minutes.

2) The device turns off automatically after the predetermined testing period. It is crucial to remember that while using a cyclic load, the frequency and intended function's form must be ascertained as a function of the applied force and time (measured in seconds). To do this, a unit known as C type is used. Figures 2 and 3 illustrate how the mathematical shape and the function in actuality differ slightly. It is important to note that the manual movement only makes minor adjustments, such as lightly touching the upper and lower footings. Prior to the test, it is used to prepare the model.

The linear variable displacement transformer (LVDT), which measures the movement beneath the shaft, was used to assess vertical settlements.

2.2.2 The model foundation

Two 20 mm thick steel foundations with various foundation diameters were used:

1) Circular footing with diameter 113 mm.

2) Square footing (100 mm ×100 mm).

Fig. 1. Control system – a general view.

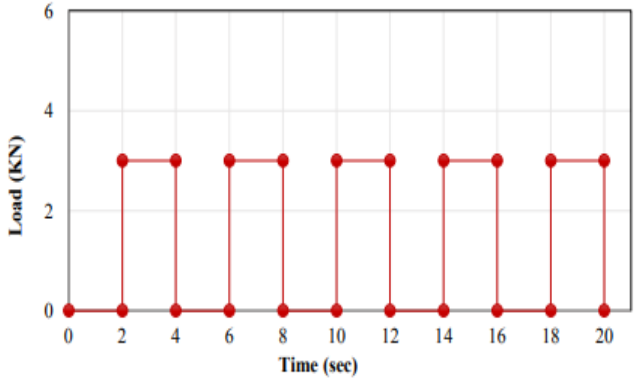

Fig. 2. Theoretical load-time relationship.

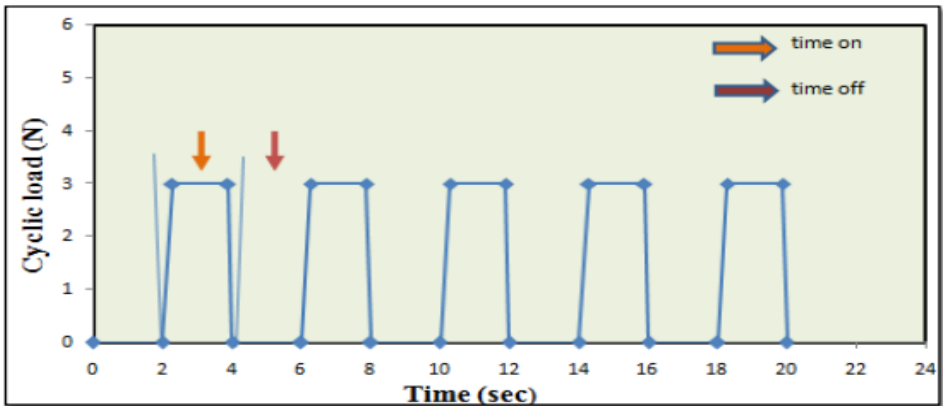

Fig. 3. Realistic load-time relationship.

2.2.3 Control tests

Trial tests were conducted to control the preparation method's efficiency prior to the stage of preparing the soil bed. Control experiments were performed to verify two key aspects of the soil bed preparation process. The first involves figuring out how shear strength changes over time at various water contents (20%, 22%, 28%, 32%, and 36%). These tests determine how long it takes the remolded soil to strengthen again after the mixing operation and a rest interval. Five samples were made separately and stacked in three layers inside molds to prove this claim. To release any trapped air, a special hammer was used to gently tap each layer.

After that, the samples were placed under a polythene sheet and kept for seven days. It was discovered that the remolded soil needs roughly five days to recover its strength. Determining how shear strength varied after five days of mixing in relation to various liquidity metrics was the second aim. Figure 4 displays the findings of the undrained shear strength fluctuation with various liquidity indices. Every day, the portable vane shear equipment was used to test the undrained shear strength. As the value of the liquidity index rises, the soil's shear strength falls.

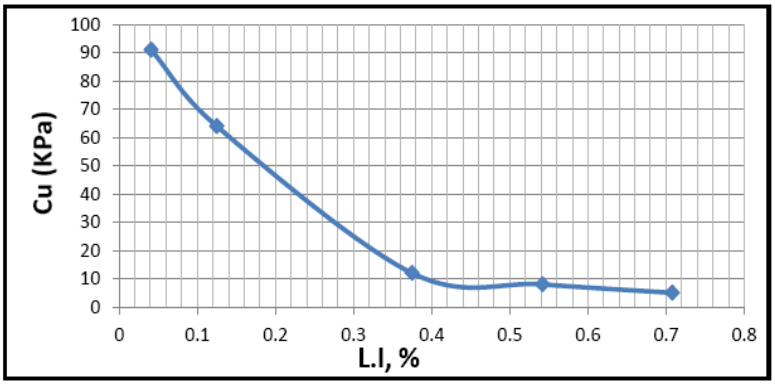

Fig. 4. Variation of the undrained shear strength with liquidity index after 5- day curing.

2.3 Tool for measuring shear strength

The "Producing ring Penetrometer" laboratory instrument, which ELE manufactures for the production of laboratory instruments, is where the concept for this device originated, as Figure 5 illustrates. An apparatus including a mirror featuring a 60° cone apex angle, 24 mm in length, and a 30 mm diameter and 141.8 mm length shank was produced. During the testing, the gadget is utilized to measure the employed clay's undrained shear strength at each loading cycle. It is linked to the hydraulic cylinder system by means of the grooves that enable installation within the machine construction, as illustrated in Figure 6.

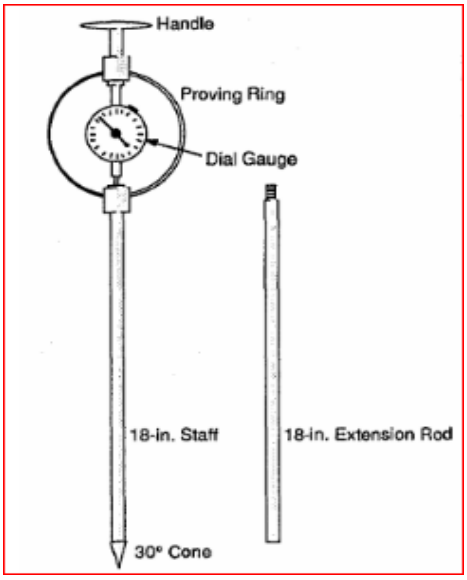

Fig. 5. Proving ring Penetrometer for measurement of soil penetration.

Fig. 6. Measuring device for soil shear resistance.

The applied static load was measured using a compression/tension load cell "SEWHA" model S-beam type (SS300), which was connected to a digital weighing indicator to read and display the load measurement. The load amount, with an input sensitivity of 0.2 μV/digit, the load cell excitation DC 10 V ± 5 V, with maximum, and the signal input voltage of 32 mV were shown using a digital weighing indicator, model SI (4010).

3. Results and discussion

3.1 Results of model testing under cyclic load

A total of 39 model experiments were conducted utilizing three distinct undrained shear strengths (20 kPa, 40 kPa, and 70 kPa), which correspond to soft, medium, and stiff clay, respectively, on clay soil as a reference under cyclic stress. The tangent suggestion is shown to be the most appropriate approach for all model testing, and it is used in this study to determine the final bearing capacity for every model.

To select the value of the applied load on the footing model, the theoretical ultimate bearing capacity of the footing was calculated according to the variables; undrained shear strength, depth of foundation, width of foundation and shape of foundation. The calculations were made based on Hansen equation [25]:

Together with the load used in the trials, Table 2 displays the findings of the vane shear device's measurements of qult, qall, and undrained shear strength (Cu). Keep in mind that the safety factor is 2.5.

Table 2. An overview of the theoretical static bearing capacity calculations.

Type of foundation	State of soil	Undrained shear strength (cu), kPa	D_f (mm)	q_{ult} (kPa), (Theoretical)	Q_{all} (N), (Theoretical)	Load applied (N)
Square	soft	20	0	123.36	493.44	246.72
			50	144.703	578.812	246.72
	medium	40	0	246.72	986.88	493.44
			50	288.623	1154.492	493.44
	stiff	70	0	431.76	1727.04	863.52
			50	504.503	2018.012	863.52
Circular	soft	20	0	123.36	494.85	246.72
			50	142.337	570.984	246.72
			100	161.315	647.116	246.72
	medium	40	0	246.72	989.72	493.44
			50	283.892	1138.834	493.44
			100	321.065	1287.951	493.44
	stiff	70	0	431.76	1732	863.52
			50	496.224	1990.602	863.52
			100	560.688	2249.203	863.52

3.2 The impact of loading rate on settlement

Figures 7 through 9 show how the rate of loading affects things. The findings show that for all rates of loading, the settlement rose in proportion to the rate of loading in all soil conditions. It is evident that the behavior of increasing settlement is same for both square and circular footings. The only cases where the settlement increased suddenly at cycle 900 and later were the ones where the cu = 40 kPa, velocity was 9 mm/sec, and the footing was at the surface.

According to the findings, the maximum cyclic settlement increased by roughly (45–63%) % in soft clay, (23–32%)% in medium clay, and (29–41%)% in stiff clay when the loading rate was increased from 3 mm/sec to 9 mm/sec. The findings concur with those of Li et al. [16], who discovered that a significant reduction in the number of cycles needed to attain failure occurs when the frequency drops from 1 Hz to 0.01 Hz.

In the first cycle, the deformation rate is comparatively high, and strain quickly rises to 50–65% of the total in a brief amount of time. Once this level is reached, the deformation rate rapidly drops while strain accumulation gradually increases to 80–90%. Compared to the first stage, this duration is longer. After that, the deformation rate keeps decreasing until it almost reaches zero.

The induced cyclic shear strain amplitudes are less than the threshold shear strain amplitude, indicating that no significant particle structural breakdown occurs and, consequently, no drop in post-cycle shear strength is seen. The low values of cyclic settlement demonstrate that the clay is in the elastic phase.

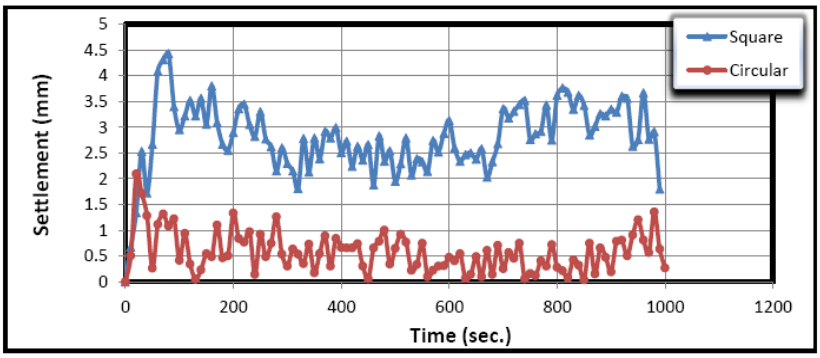

a) Loading rate = 3 mm/sec.

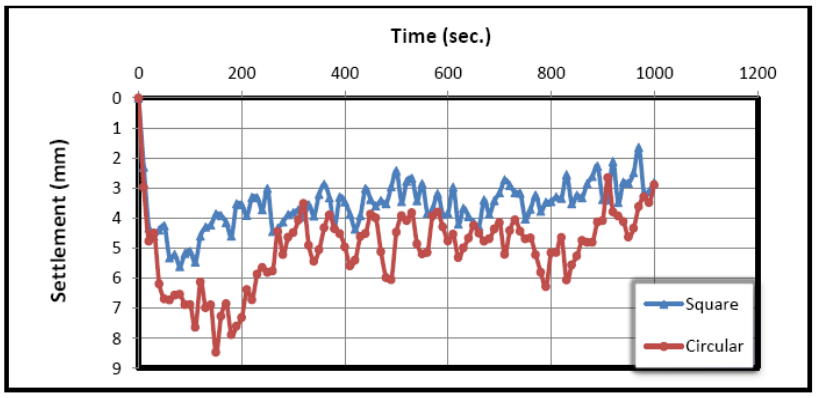

b) Loading rate =9 mm/sec.

Fig. 7. Settlement change with time when cu = 20 kPa, D_f = 0 at different rates of loading.

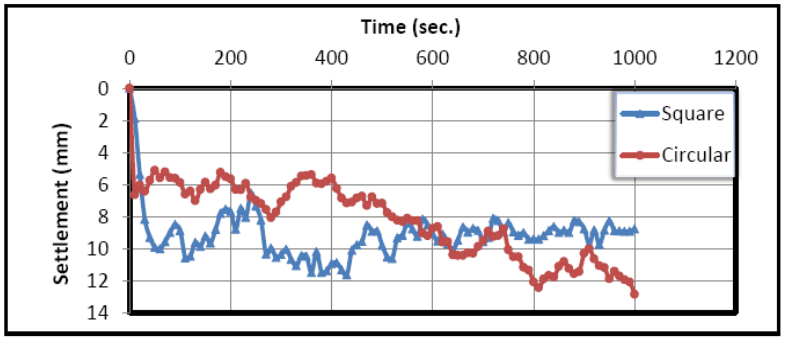

a) Loading rate =3 mm/sec.

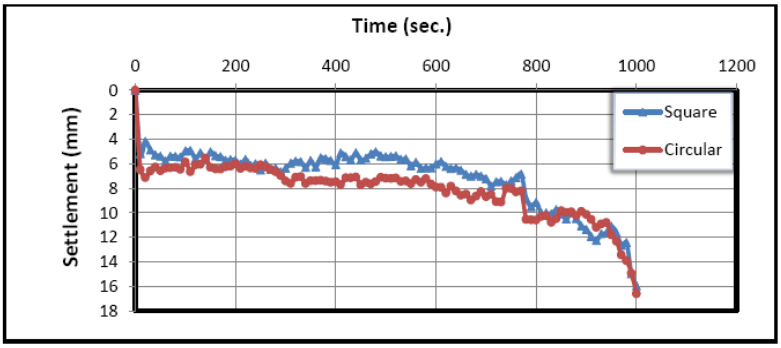

b) Loading rate =9 mm/sec.

Fig. 8. Settlement change with time when cu = 40 kPa and D_f = 0 at different rates of loading.

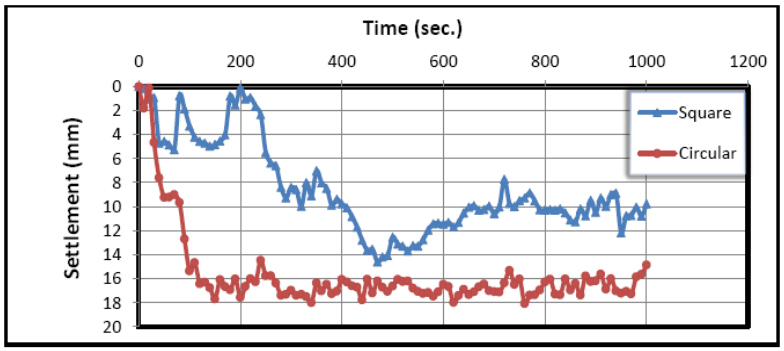

a) Loading rate =3 mm/sec.

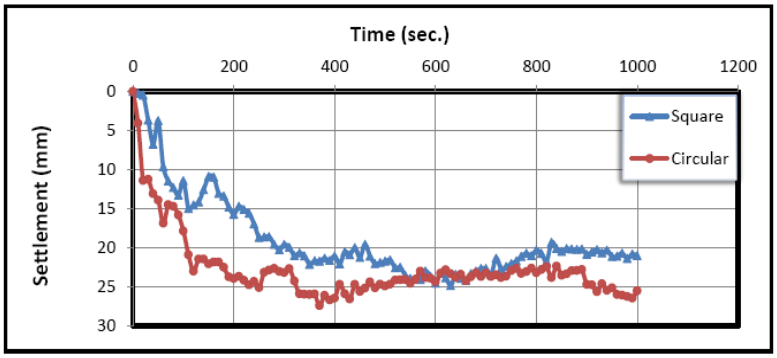

b) Loading rate =9 mm/sec.

Fig. 9. Settlement change with time when cu = 70 kPa and D_f = 0 at different rates of loading.

3.3 Evaluation of soil shear-strength after loading

An array of pre-measurements was completed in order to assess the soil's shear strength following loading. By creating soil models of eight samples at shear strengths ranging from soft (Cu = 20 kPa) to stiff (Cu = 88 kPa), the association between the reaction of soil (R) and undrained shear strength (Cu) was discovered. The eight samples' undrained shear strength was determined using a direct shear test apparatus in accordance with ASTM D3080 [26] specifications. A miniature model measuring 350 mm by 350 mm by 350 mm had a static load applied to it, and the response of the clay in these soils was monitored using a load cell and digital weighing indicator devices.

For this reason, the device's speed was set to 3 mm/sec for all measurements while a constant pressure of 2.5 bars was applied, and as Figure 10 illustrates, the minimum soil depth needed for the cone penetration was 120 mm. Table 3 presents the results of the soil reaction and the undrained shear strength for the eight samples; Figure 11 shows the link between the soil reaction and the undrained shear strength.

The following can be used to express the relationship between Figure 11's undrained shear strength and soil response (R):

$$Cu = q_0(1 + \frac{bx}{a})^{(\frac{-1}{b})} \quad (1)$$

where, q_o = 6.0641 x 10^{-2} , a = - 2.3939 x 10^{-2} and b = - 1.3719.

The coefficient of determination (R^2) = 98.13

The data obtained with the Curve Expert Professional Properties Program fits the relationship shown above.

Fig. 10. Manufactured apparatus for measurement of soil strength.

Table 3. Results of the soil reaction and the undrained shear strength.

Test No.	W.C%	Cu (kN/m^2)	Reaction of soil, R (N)
1	22	88	407
2	24	82	320
3	26	64	211.5
4	28	50	156.5
5	30	42	169
6	32	37	122
7	34	32	99
8	36	20	57

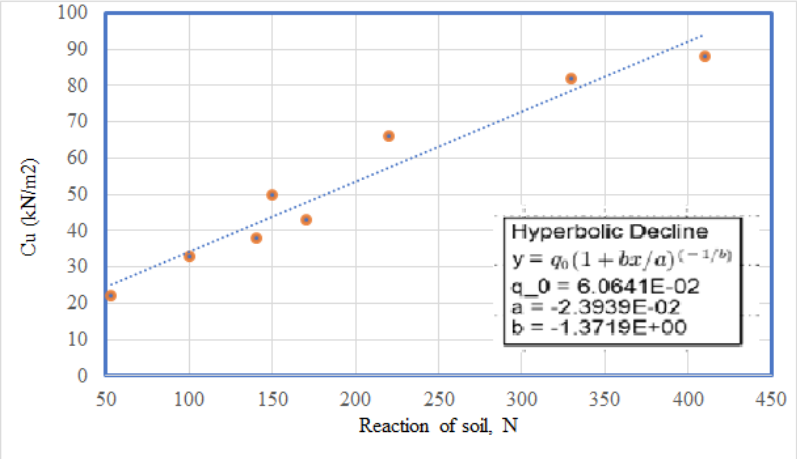

Fig. 11. Relationship between the soil reaction and the undrained shear strength.

3.4 Clay's shear strength following a cyclic load

Numerous laboratory and field experiments can be used to determine the saturated clay specimen's undrained shear strength. These tests all require that the failure stresses be developed without any changes to volume or drainage. Also, relatively undisturbed soil must be used for testing. The following are the main assessments utilized in the current practice:

1) Laboratory tests, including triaxial and unconfined compression tests.

2) In situ examinations: cone penetration and vane shear testing.

Following the cyclic load test of each model, the undrained shear strength of the clay was measured using the constructed device. After the test, the cone and shank are subjected to a constant static load of 468.75 N (2.5 bar) at a velocity of 3 mm/sec. A load cell is then used to measure the soil's reaction when the penetration of the cone and shank reaches 112 mm. This method yields the undrained shear strength. The variation in the rise of the undrained shear strength following testing of several footing models is shown in Figure 12 and Table 4.

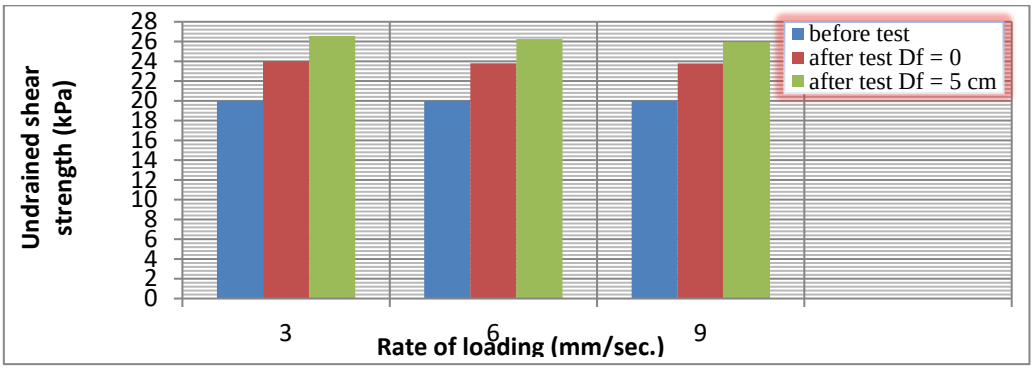

a. Cu = 20 kPa and square footing.

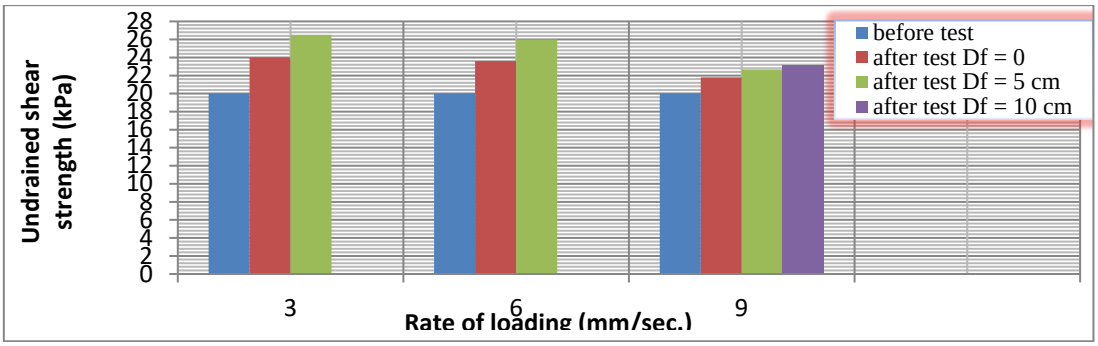

b. Cu = 20 kPa and circular footing.

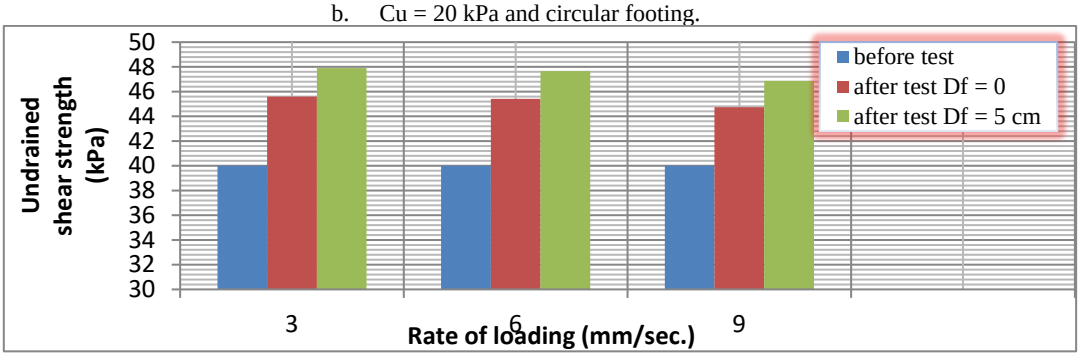

c. Cu = 40 kPa and square footing.

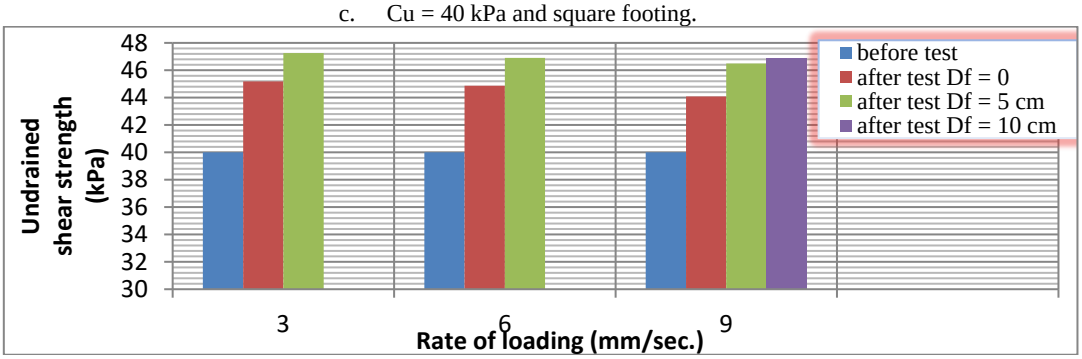

d. Cu = 40 kPa and circular footing.

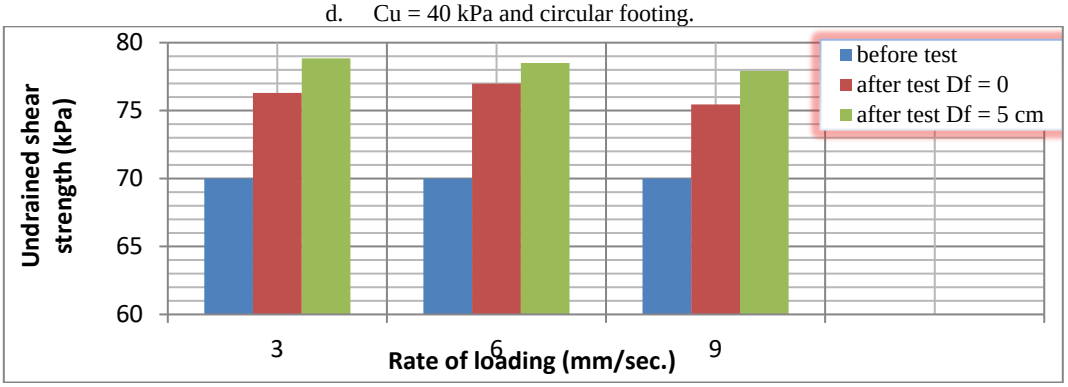

e. Cu = 70 kPa and square footing.

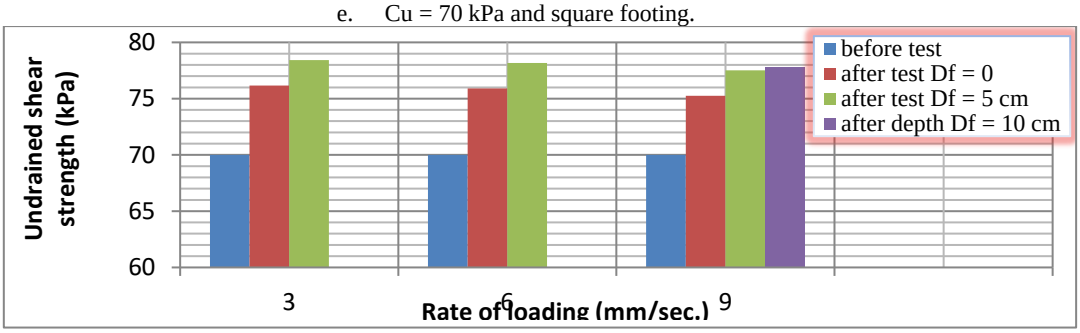

f. Cu = 70 kPa and circular footing.

Fig. 12. Variation of the value of undrained shear strength with the rate of loading during cyclic load test.

Table 4. The undrained shear strength values both prior to and following load cycles.

		Depth of footing (cm)	c_u before test = 20 kPa	c_u before test = 40 kPa	c_u before test = 70 kPa
Velocity (3 mm/sec)	Square footing	At surface	24	45.6	76.3
		$D_f = 5$	26.58	47.9	78.85
		$D_f = 10$	-	-	-
	Circular footing	At surface	23.99	45.19	76.17
		$D_f = 5$	26.51	47.26	78.43
		$D_f = 10$	-	-	-
Velocity (6 mm/sec)	Square footing	At surface	23.8	45.41	76.98
		$D_f = 5$	26.25	47.65	78.5
		$D_f = 10$	-	-	-
	Circular footing	At surface	23.6	44.87	75.91
		$D_f = 5$	26	46.9	78.17
		$D_f = 10$	-	-	-
Velocity (9 mm/sec)	Square footing	At surface	23.79	44.74	75.45
		$D_f = 5$	25.9	46.87	77.91
		$D_f = 10$	-	-	-
	Circular footing	At surface	21.79	44.09	75.25
		$D_f = 5$	22.66	46.5	77.52
		$D_f = 10$	23.12	46.90	77.81

Overall, the results show that the soil's undrained shear strength increased following the cyclic load test compared to its pre-test value; however, the degree of this increase varied depending on the variables.

According to Kawa et al. [27], reinforced soils were less sensitive to the number of loading applications than ordinary soil (no column) for models of soft soil reinforced by stone column subjected to cyclic load below the threshold loading rate 5 mm/sec.

This is because loading causes the column materials to compact, increasing their density and resulting in a higher resistance to deformation and, ultimately, less settlement. Models evaluated at a loading rate of 5 mm/sec were not able to reach the failure level as quickly as models subjected to cyclic loading at a loading rate of 10 mm/sec. This was also provided by Najim et al. [28].

4. Conclusions

The following points were outlined:

1) The maximum cyclic settlement increased by roughly (45–63%)% in soft clay, (23–32%)% in medium clay, and (29–41%)% in stiff clay when the loading rate was increased from 3 mm/sec to 9 mm/sec.

2) At the start of the test, there was a sharp rise in settlement. This indicates that in all models, the threshold stain is extremely tiny in the zones of cyclic amplitudes.

3) The increase in undrained shear strength increases with increasing footing depth.

4) The value of the increase in the undrained shear strength increases with decreasing loading rate.

5) When the shape of the footing changes, utilizing square footing results in a higher rise in the undrained shear strength than using circular footing.

5. References

[1] Bray J D, Sancio R B, Durgunoglu T, Onalp A, Seed R B, Stewart J P, Youd T L, Baturay M B, Cetin O K, Christensen C, Karadayilar T, Emrem C. Ground failure in Adapazari, Turkey, 15th ICSMGE, TC4 Satellite Conference on Lessons Learned from Recent Strong Earthquakes. August 1, 2011, Istanbul, Turkey, pp. 19–28.

[2] Bray J D, Sancio R B, Durgunoglu T, Onalp A, Youd T L, Stewart J P, Seed R B, Cetin O K, Bol E, Baturay M B, Christensen C, Karadayilar. Subsurface characterization at ground failure sites in Adapazari, Turkey. Journal of Geotechnical and Geoenvironmental Engineering, 2004; 130 (7): 673–685.

[3] Seed H B, Martin P P, Lysmer J. Pore water pressure changes during liquefaction. Journal of Soil Mechanics and Foundations Division. 1976; 102: 323–347.

[4] Vaid Y P. Liquefaction of silty soils. Ground failures under seismic conditions: Proceedings of the sessions sponsored by the Geotechnical Engineering Division of the ASCE in conjunction with the ASCE National Convention in Atlanta Georgia. October 9–13, New York: ASCE, Geotechnical Special Publication, No. 44,

1994.
[5] Fattah M Y, Al-Mosawi M J, Al-Ameri A F I. Stresses and Pore Water Pressure Induced by Machine Foundation on Saturated Sand. Ocean Engineering. 2017;146:268–281. https://doi.org/10.1016/j.oceaneng.2017.09.055.
[6] El Hosri M S, Biarez H, Hicher P Y. Liquefaction characteristics of silty clay. Proc. Eight World Conference on Earthquake Engineering, Prentice Hall, N.J., 1984, pp. 277–284.
[7] Zhu R, Law K T. Liquefaction potential of silt. Proceedings of Ninth International Conference on Earthquake Engineering, Tokyo–Kyoto, Japan, 1988, pp. 237–242.
[8] Erken A, Ansal A M. Liquefaction characteristic of undisturbed sands. Performance of Ground and Soil Structures, Thirteenth International Conference on Soil Mechanics and Foundation Engineering, 1994, pp. 165–170.
[9] Puri V K. Liquefaction behavior and dynamic properties of loessial (silty) soils. Ph.D. Thesis, 1984, University of Missouri-Rolla, UMI, Ann Arbor.
[10] Ansal A M, Erken. Undrained behavior of clay under cyclic shear stresses, Journal of the Geotechnical Engineering Division. 1989; 115: 968–983.
[11] Boulanger R W, Idriss I M. Evaluating the potential for liquefaction or cyclic failure of silts and clays. Center for Geotechnical Modeling, Report No. UCD/CGM-04/01. Department of Civil and Enviromental Engineering, College of Engineering, University of California, Davis, 2004.
[12] Koester J P. Cyclic strength and pore pressure generation characteristics of fine-grained soils. Ph.D. Thesis, 1992, University of Colorado at Boulder, UMI, Ann Arbor.
[13] Finn W D L. Dynamic analysis and liquefaction-emerging trends. Proc. Third Int. Earth. Micr. Conf., Seattle, Washington, 1982, pp. 909–929.
[14] Vasquez-Herrera A, Dobry R. Re-evaluation of the lower San Fernando Dam. Report-3: The Behavior of Undrained Contractive Sand and its Effect on Seismic Liquefaction Flow Failures of Earth Structures. Contract Report GL-89-2. US Army Waterways Experiment Station, Vicksburg, MS, 1989.
[15] Marcuson W F, Hynes M E, Franklin A G. Evaluation and use of residual strength in seismic safety analysis of embankments. Earthquake Spectra. 1990;6: 529–572.
[16] Li L I, Han-bo D, Wang L Z, Undrained behavior of natural marine clay under cyclic loading. Ocean Engineering. 2011; 38(16): 1792-1805.
[17] Fattah M Y, Karim H H, Al-Qazzaz H H. Cyclic behavior of footings on dry sand under different rates of loading, International Journal of Construction Engineering and Management. 2017; 6(6):240-253, DOI: 10.5923/j.ijcem.20170606.03.
[18] Fattah M Y, Aladili A S, Yousif H F. Investigation of reinforced sub-base layer on saturated expansive subgrade soil under cyclic loading. International Journal of Earth Sciences and Engineering. 2017;10(3): 604-615. DOI:10.21276/ijee.2017.10.0319.
[19] Ren X, Xu Q, Teng J, Zhao N, Lv. A novel model for the cumulative plastic strain of soft marine clay under long-term low cyclic loads. Ocean Engineering. 2017; 149:194-204.
[20] Patiño H, Galindo R and Marañón C O. Cyclic and Permanent Shear Strains of a Soft Cohesive Soil Subjected to Combined Static and Cyclic Loading. Applied Sciences. 2020;10: 8433. doi:10.3390/app10238433.
[21] Thakur A S, Pandya S & Sachan A. Dynamic behavior and characteristic failure response of low plasticity cohesive soil. Int J Civ Eng. 2021;19: 167–185. https://doi.org/10.1007/s40999-020-00560-1
[22] ASTM D 4318, Standard Test Method for Liquid Limit, Plastic Limit, and Plasticity Index of Soil, American Society for Testing and Materials (ASTM).
[23] ASTM D 854, Standard Test Method for Specific Gravity, American Society for Testing and Materials (ASTM).
[24] ASTM D 422, Standard Test Method for Particle Size Analysis of Soils, American Society for Testing and Materials (ASTM).
[25] Hansen, J. B. A Revised and Extended Formula for Bearing Capacity. Geoteknisk Instutut (Danish Geotechnical Institute), Bulletin No. 28, pp. 5–11. 1970.
[26] ASTM D3080, Standard Test Method for Direct Shear Test of Soils under Consolidated Drained Conditions, American Society for Testing and Materials (ASTM).
[27] Kawa S F, Fattah M Y, Kolosov E S. Behavior of foundation soil improved by stone column under cyclic load. MATEC Web of Conferences 2018;239:05015. https://doi.org/10.1051/matecconf/201823905015.
[28] Najim A N, Fattah M Y, Al-Recaby M K M, Cyclic settlement of footings of different shapes resting on clayey soil. Engineering and Technology Journal. 2020; 38(3A): 465-477.